

# Can the Differential Emission Measure constrain the timescale of the energy deposition in the solar corona ?

Application to Hinode/EIS

Chloé Guennou<sup>1</sup>

[chloe.guennou@ias.u-psud.fr](mailto:chloe.guennou@ias.u-psud.fr)

F. Auchère<sup>1</sup>, J.A. Klimchuk<sup>2</sup>, E. Soubrié<sup>1</sup>,  
K. Bocchialini<sup>1</sup>, S. Parenti<sup>3</sup>



**Goddard**  
SPACE FLIGHT CENTER

<sup>1</sup> Institut d'Astrophysique spatiale, Bât 121, 91400 Orsay, France

<sup>2</sup> NASA Goddard Space Flight Center, Heliophysics Science Division , Greenbelt, MD

<sup>3</sup> Royal Observatory of Belgium, avenue Circulaire 3, 1180, Brussels, Belgium



## ■ Why ?

➤ Active Region → **DEM  $\propto T^\alpha$**

(Warren et al. 2011, Winebarger et al. 2012, Schmelz 2012 ...)

➤ **Slope** determination :

- Indication of the **cold/warm** material ratio

- **Timescale** of the energy deposition in the solar corona

# ■ Introduction

- I. Technique
- II. Results
- Conclusions

## ■ Why ?



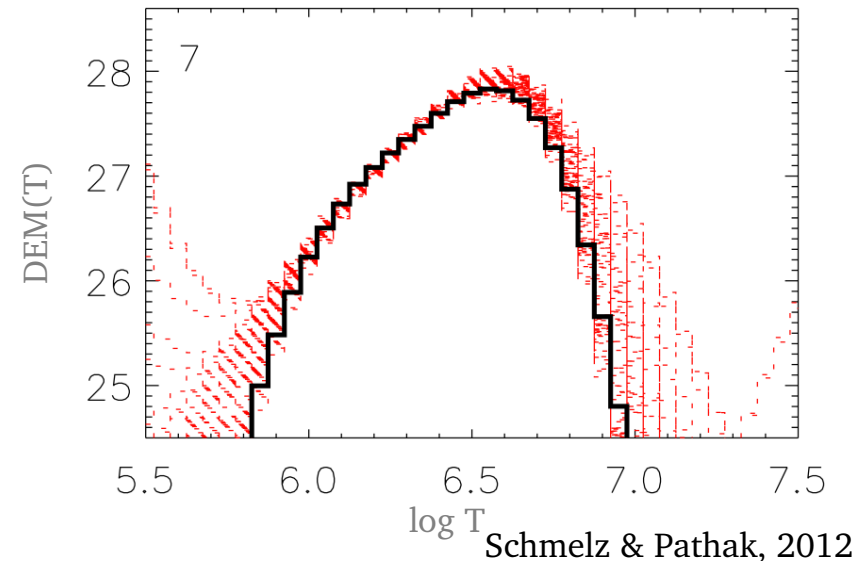
➤ Active Region →  $\text{DEM} \propto T^\alpha$

(Warren et al. 2011, Winebarger et al. 2012, Schmelz 2012 ...)

➤ **Slope** determination :

→ Indication of the **cold/warm** material ratio

→ **Timescale** of the energy deposition in the solar corona



# ■ Introduction

- I. Technique
- II. Results
- Conclusions

## ■ Why ?



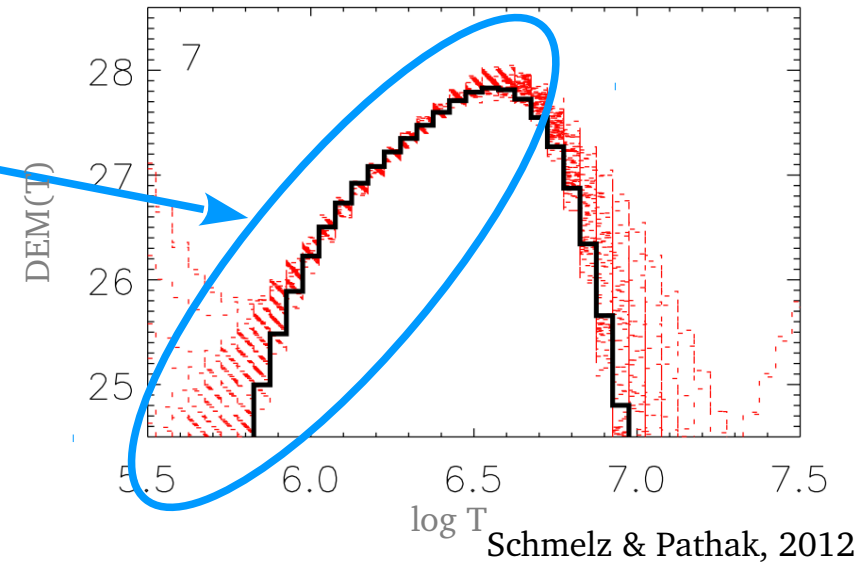
➤ Active Region →  $\text{DEM} \propto T^\alpha$

(Warren et al. 2011, Winebarger et al. 2012, Schmelz 2012 ...)

➤ **Slope** determination :

→ Indication of the **cold/warm** material ratio

→ **Timescale** of the energy deposition in the solar corona



# ■ Introduction

- I. Technique
- II. Results
- Conclusions

## ■ Why ?



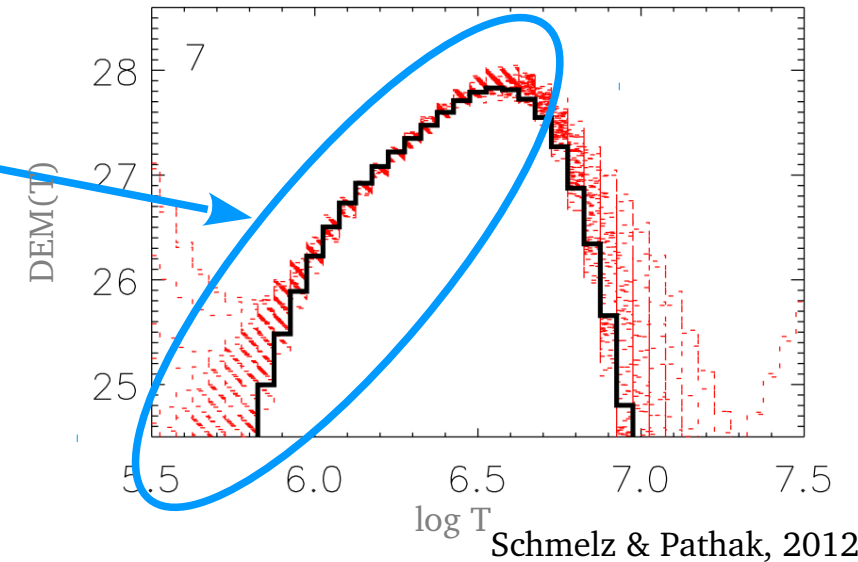
➤ Active Region →  $\text{DEM} \propto T^\alpha$

(Warren et al. 2011, Winebarger et al. 2012, Schmelz 2012 ...)

➤ **Slope** determination :

→ Indication of the **cold/warm** material ratio

→ **Timescale** of the energy deposition in the solar corona



■ **But ...**



DEM → Inverse problem

# ■ Introduction

- I. Technique
- II. Results
- Conclusions

## ■ Why ?



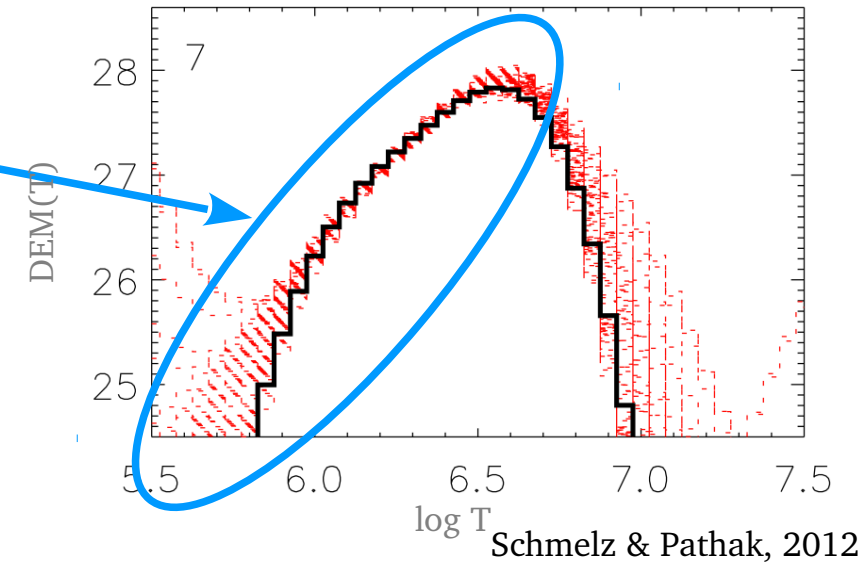
➤ Active Region → DEM  $\propto T^\alpha$

(Warren et al. 2011, Winebarger et al. 2012, Schmelz 2012 ...)

➤ **Slope** determination :

→ Indication of the **cold/warm** material ratio

→ **Timescale** of the energy deposition in the solar corona



■ **But ...**



DEM → Inverse problem

$$I_b = \frac{1}{4\pi} \int_0^\infty R_b(T_e) \xi(T_e) dT_e$$



# ■ Introduction

- I. Technique
- II. Results
- Conclusions

## ■ Why ?



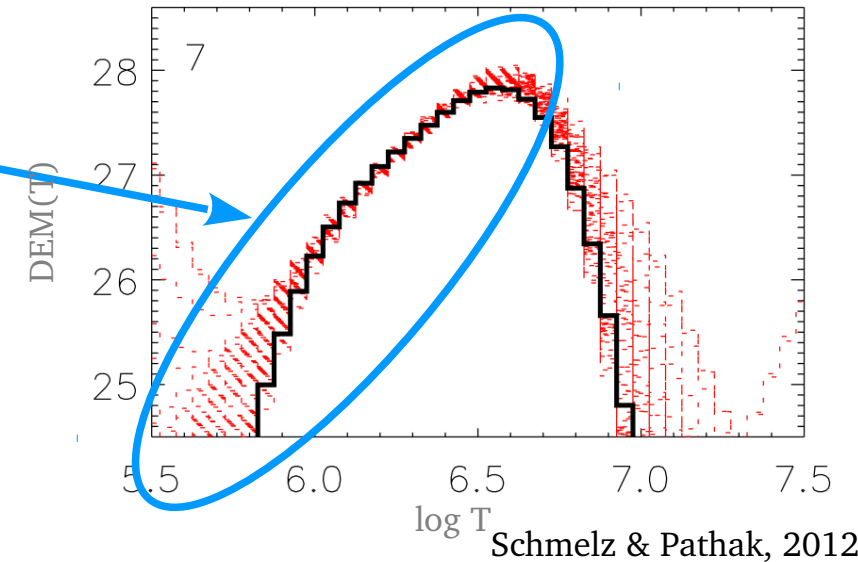
➤ Active Region → DEM  $\propto T^\alpha$

(Warren et al. 2011, Winebarger et al. 2012, Schmelz 2012 ...)

➤ Slope determination :

→ Indication of the **cold/warm** material ratio

→ **Timescale** of the energy deposition in the solar corona



■ But ...



DEM → Inverse problem

$$I_b = \frac{1}{4\pi} \int_0^\infty R_b(T_e) \xi(T_e) dT_e$$

Temperature Response function



# ■ Introduction

- I. Technique
- II. Results
- Conclusions

## ■ Why ?



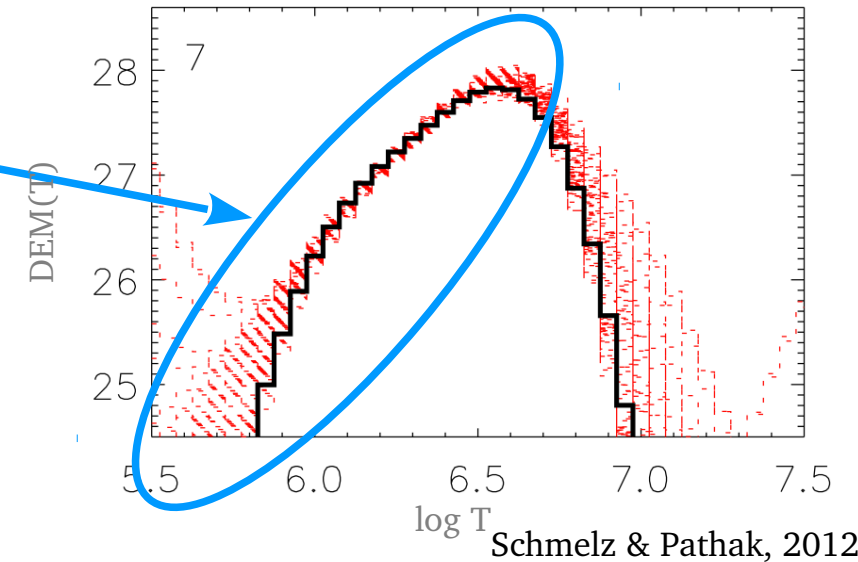
➤ Active Region → DEM  $\propto T^\alpha$

(Warren et al. 2011, Winebarger et al. 2012, Schmelz 2012 ...)

➤ Slope determination :

→ Indication of the **cold/warm** material ratio

→ **Timescale** of the energy deposition in the solar corona



■ But ...

➡ DEM → Inverse problem

$$I_b = \frac{1}{4\pi} \int_0^{\infty} R_b(T_e) \xi(T_e) dT_e$$

Temperature Response function

DEM function

$$\xi(T_e) = \overline{n_e^2}(T_e) dp/d(\log T_e),$$

Craig & Brown (1976)



# ■ Introduction

- I. Technique
- II. Results
- Conclusions

## ■ Why ?



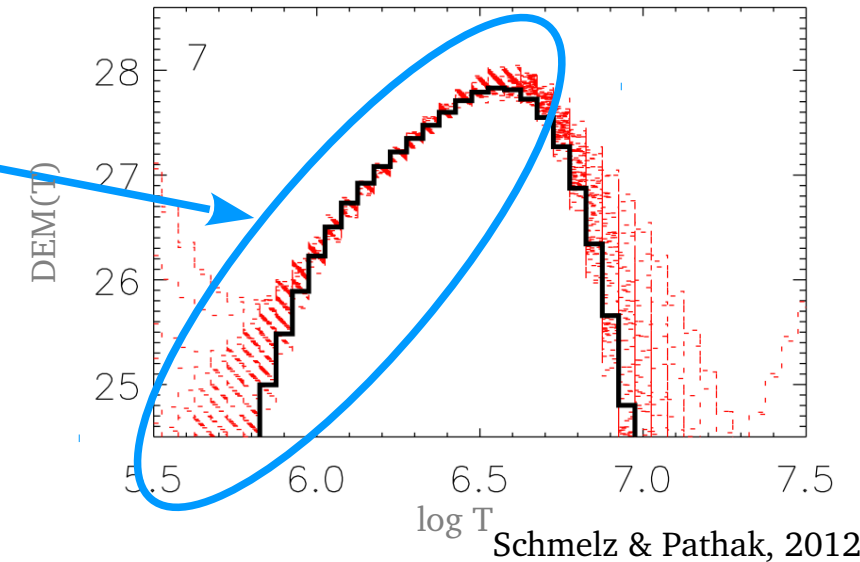
➤ Active Region → DEM  $\propto T^\alpha$

(Warren et al. 2011, Winebarger et al. 2012, Schmelz 2012 ...)

➤ Slope determination :

→ Indication of the cold/warm material ratio

→ Timescale of the energy deposition in the solar corona



■ But ...

DEM → Inverse problem

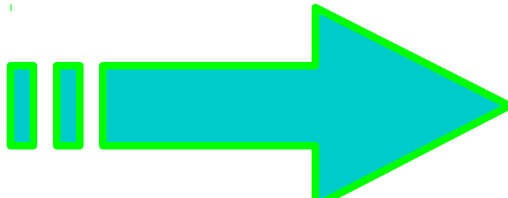
$$I_b = \frac{1}{4\pi} \int_0^{\infty} R_b(T_e) \xi(T_e) dT_e$$

Temperature Response function

DEM function

$$\xi(T_e) = \overline{n_e^2}(T_e) dp/d(\log T_e),$$

Craig & Brown (1976)



What is the confidence level on the reconstructed slope ?

 How ?

➤ Technique → *Monte-carlo treatment* of uncertainties

**Hinode/EIS set of 30 lines of *Fe, Si, Mg, S, Ca, Ar***  
→ temperature range  $[10^{5.2}: 10^{6.9}]$  K

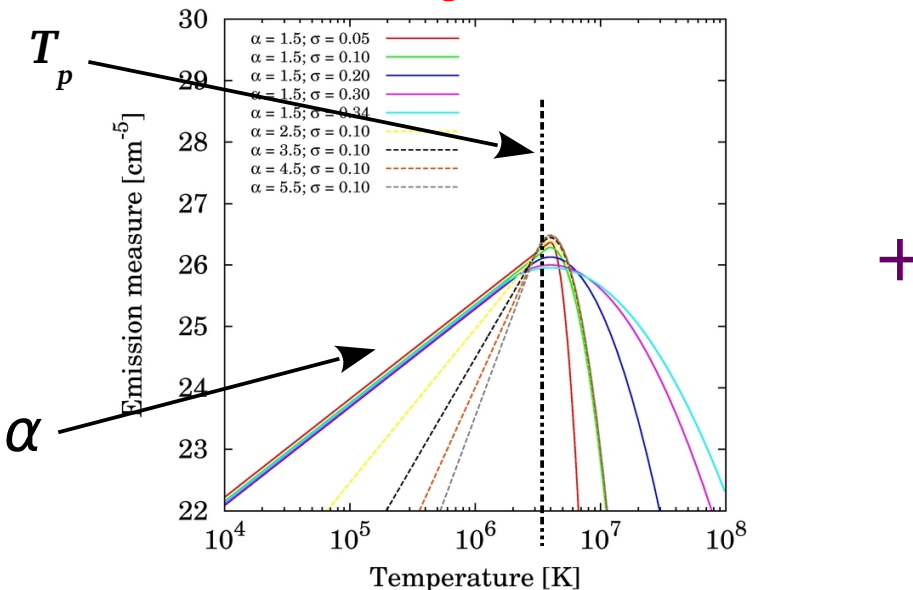


# ■ How ?

➤ Technique → *Monte-carlo treatment* of uncertainties

**Hinode/EIS set of 30 lines of *Fe, Si, Mg, S, Ca, Ar***  
 → temperature range  $[10^{5.2}: 10^{6.9}]$  K

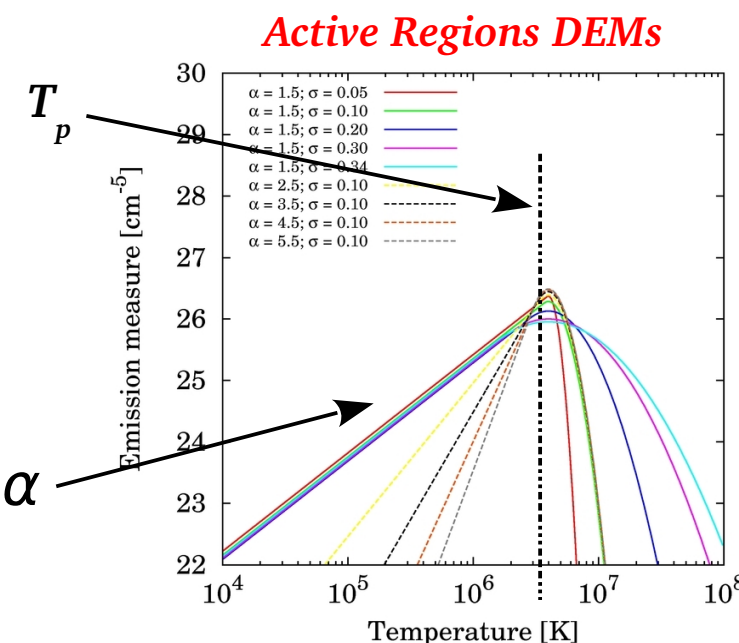
## Active Regions DEMs



 How ?


➤ Technique → *Monte-carlo treatment* of uncertainties

**Hinode/EIS set of 30 lines of *Fe, Si, Mg, S, Ca, Ar***  
 → temperature range  $[10^{5.2} : 10^{6.9}] \text{ K}$



$$\xi^I = \arg \min \left[ \sum_{b=1}^{N_b} \left( \frac{I_b^{obs}(\xi^P) - I_b^{th}(\xi)}{\sigma_b^u} \right)^2 \right]$$

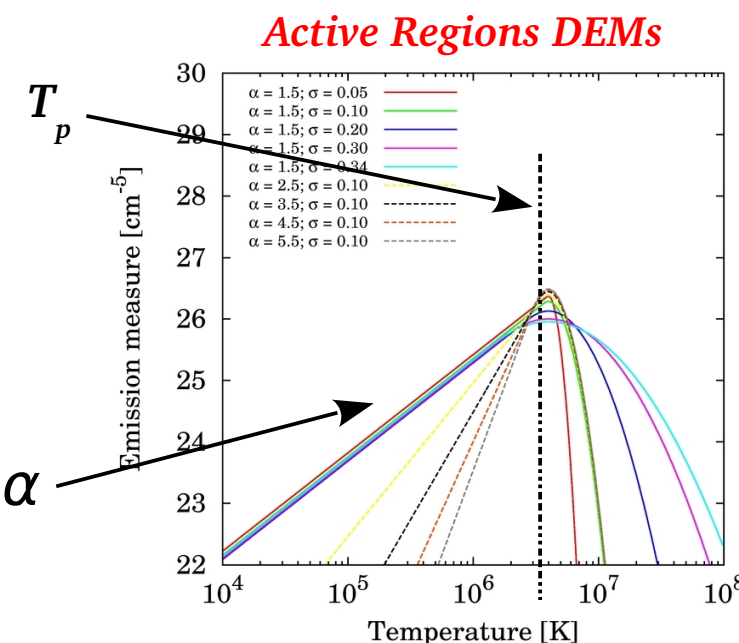
+

(Guennou et al. 2012, part I and II)

# ■ How ?

➤ Technique → *Monte-carlo treatment* of uncertainties

**Hinode/EIS set of 30 lines of *Fe, Si, Mg, S, Ca, Ar***  
 → temperature range  $[10^{5.2}: 10^{6.9}]$  K



$$\xi^I = \arg \min \left[ \sum_{b=1}^{N_b} \left( \frac{I_b^{obs}(\xi^P) - I_b^{th}(\xi)}{\sigma_b^u} \right)^2 \right]$$

measurement noises

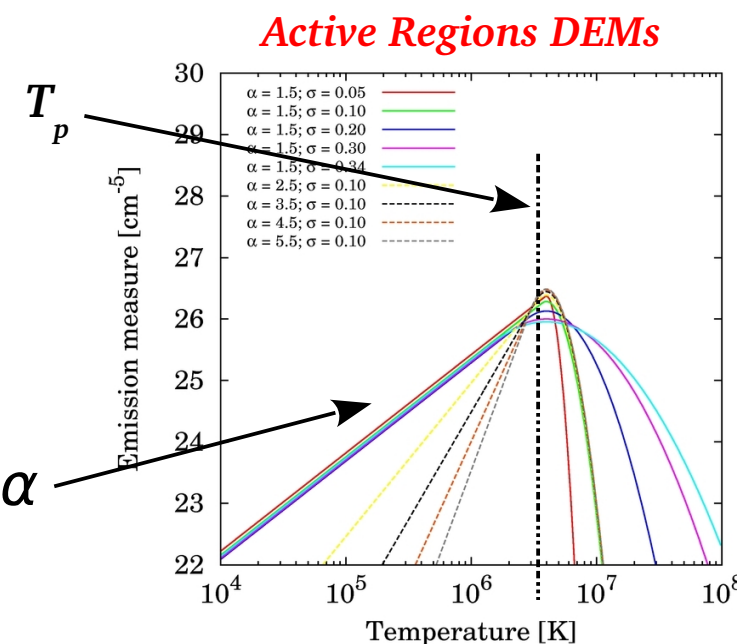
+

(Guennou et al. 2012, part I and II)

## ■ How ?

➤ Technique → *Monte-carlo treatment* of uncertainties

**Hinode/EIS set of 30 lines of *Fe, Si, Mg, S, Ca, Ar***  
 → temperature range  $[10^{5.2}: 10^{6.9}]$  K



+

$$\xi^I = \arg \min_{\xi} \left[ \sum_{b=1}^{N_b} \left( \frac{I_b^{obs}(\xi^P) - I_b^{th}(\xi)}{\sigma_b} \right)^2 \right]$$

measurement noises

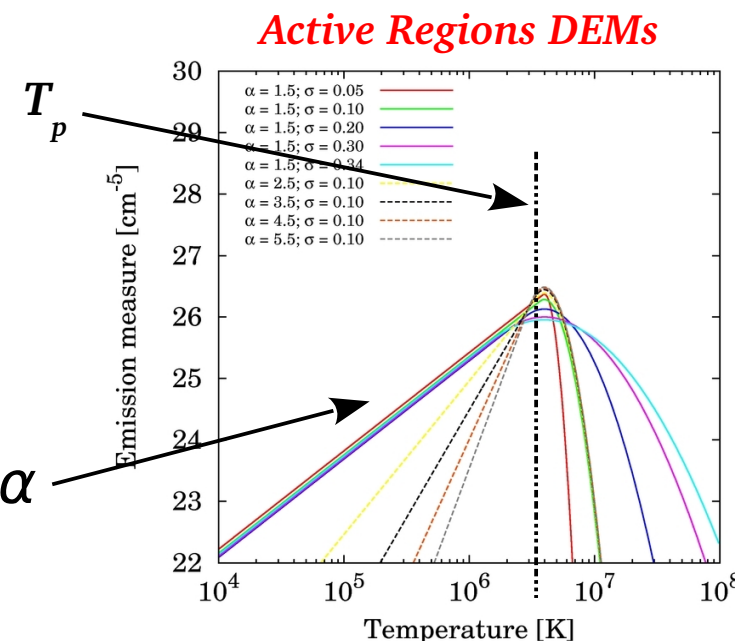
systematic errors

(Guennou et al. 2012, part I and II)

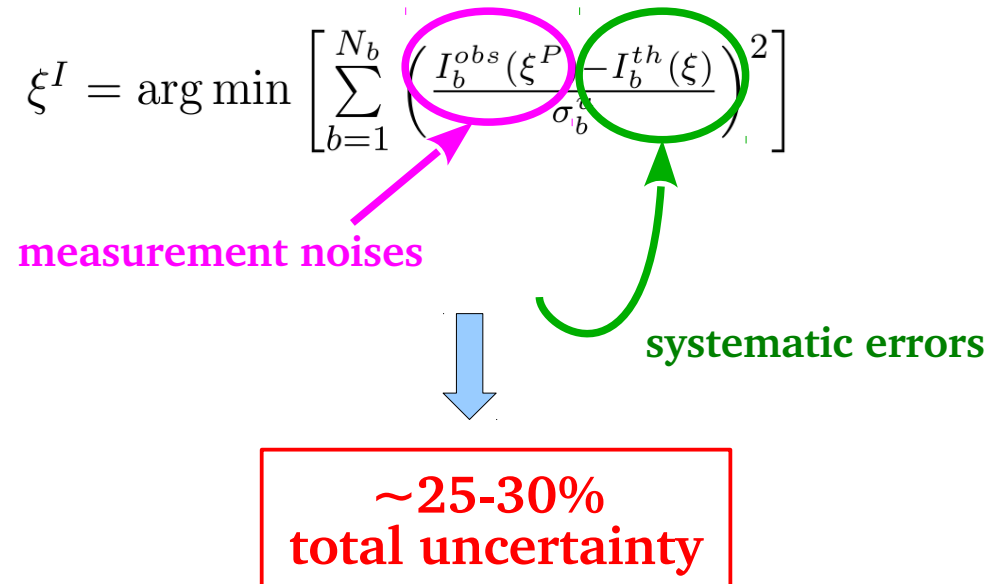
# ■ How ?

➤ Technique → *Monte-carlo treatment* of uncertainties

**Hinode/EIS set of 30 lines of *Fe, Si, Mg, S, Ca, Ar***  
 → temperature range  $[10^{5.2}: 10^{6.9}]$  K



+



(Guennou et al. 2012, part I and II)

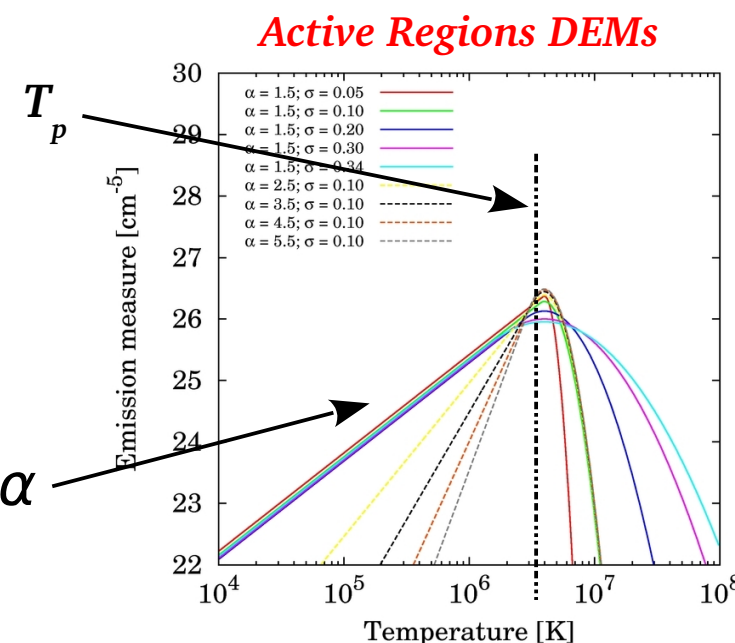
Thanks to H. Mason, E.  
 Landi, G. DelZanna, J.  
 Schmelz, H. Warren, P.  
 Young, G. Doschek



## ■ How ?

➤ Technique → *Monte-carlo treatment* of uncertainties

**Hinode/EIS set of 30 lines of *Fe, Si, Mg, S, Ca, Ar***  
 → temperature range  $[10^{5.2} : 10^{6.9}]$  K



$$\xi^I = \arg \min_{\xi} \left[ \sum_{b=1}^{N_b} \left( \frac{I_b^{obs}(\xi^P) - I_b^{th}(\xi)}{\sigma_b} \right)^2 \right]$$

+

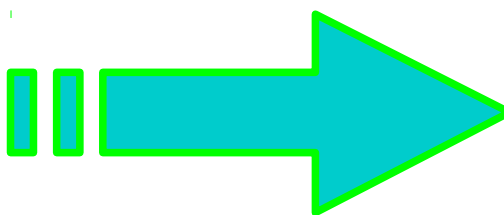
measurement noises

systematic errors

~25-30%  
total uncertainty

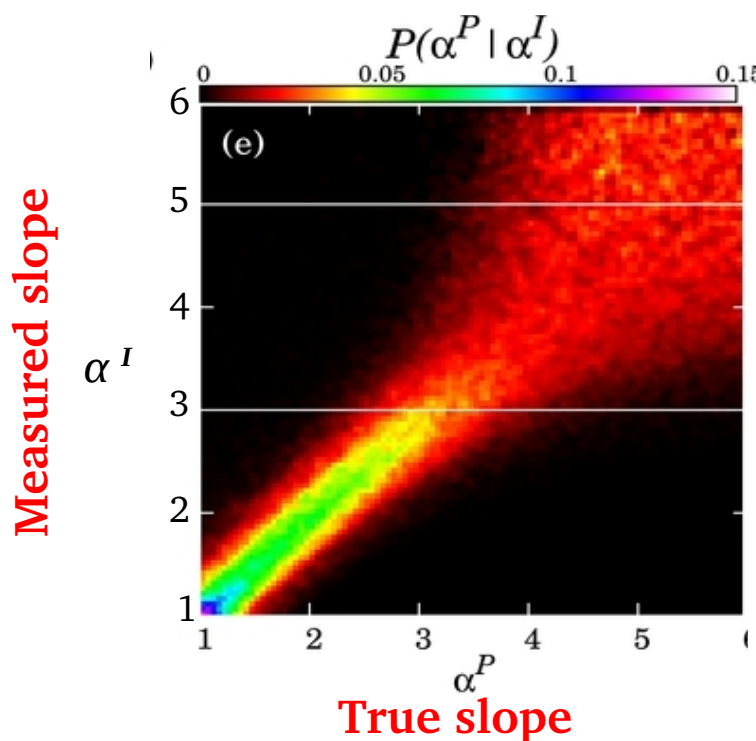
(Guennou et al. 2012, part I and II)

Thanks to H. Mason, E. Landi, G. DelZanna, J. Schmelz, H. Warren, P. Young, G. Doschek



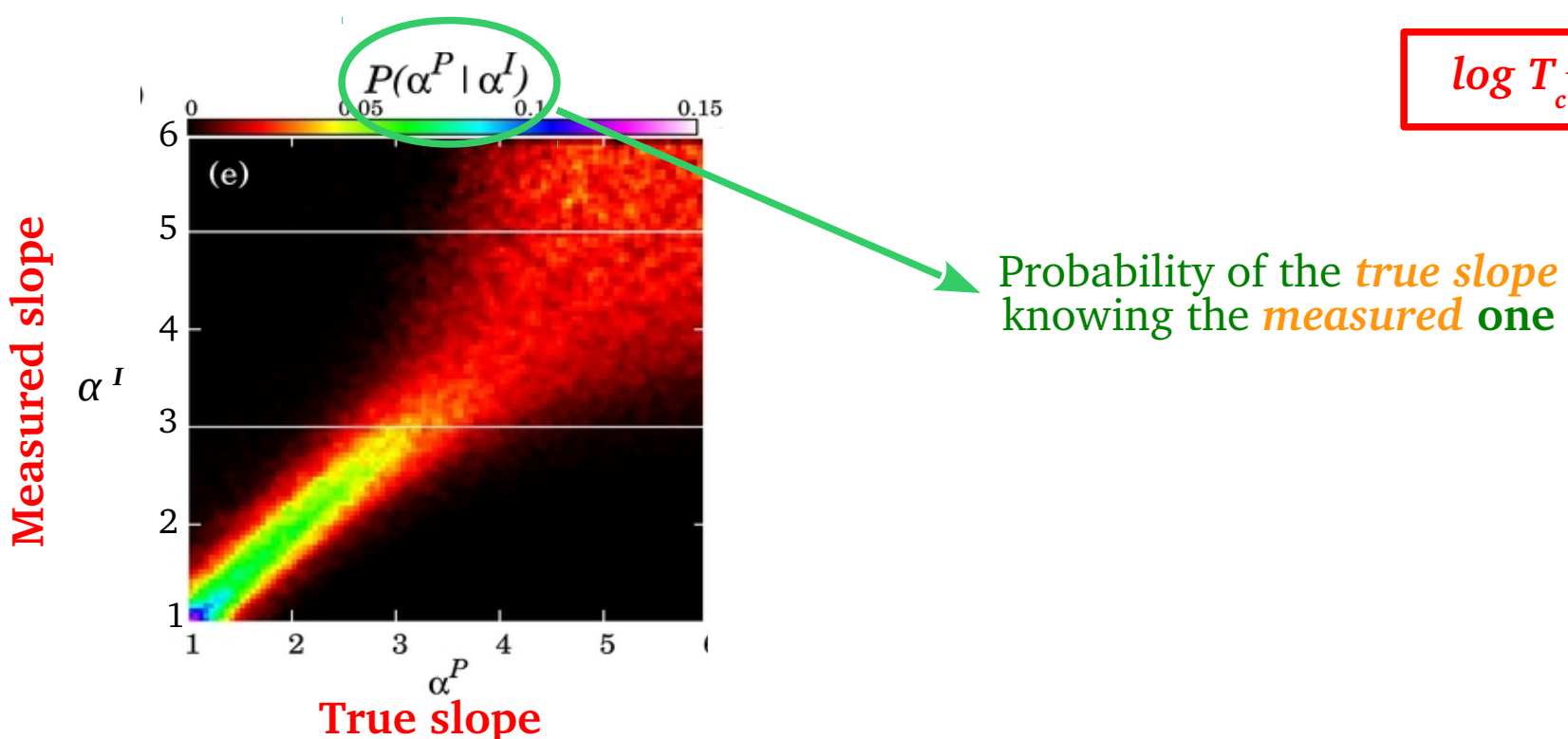
Compute *all the solutions consistent with the data*  
 + associated probabilities  
 → *to derive confidence level on the estimated slopes*

## ■ Reconstruction of the slope



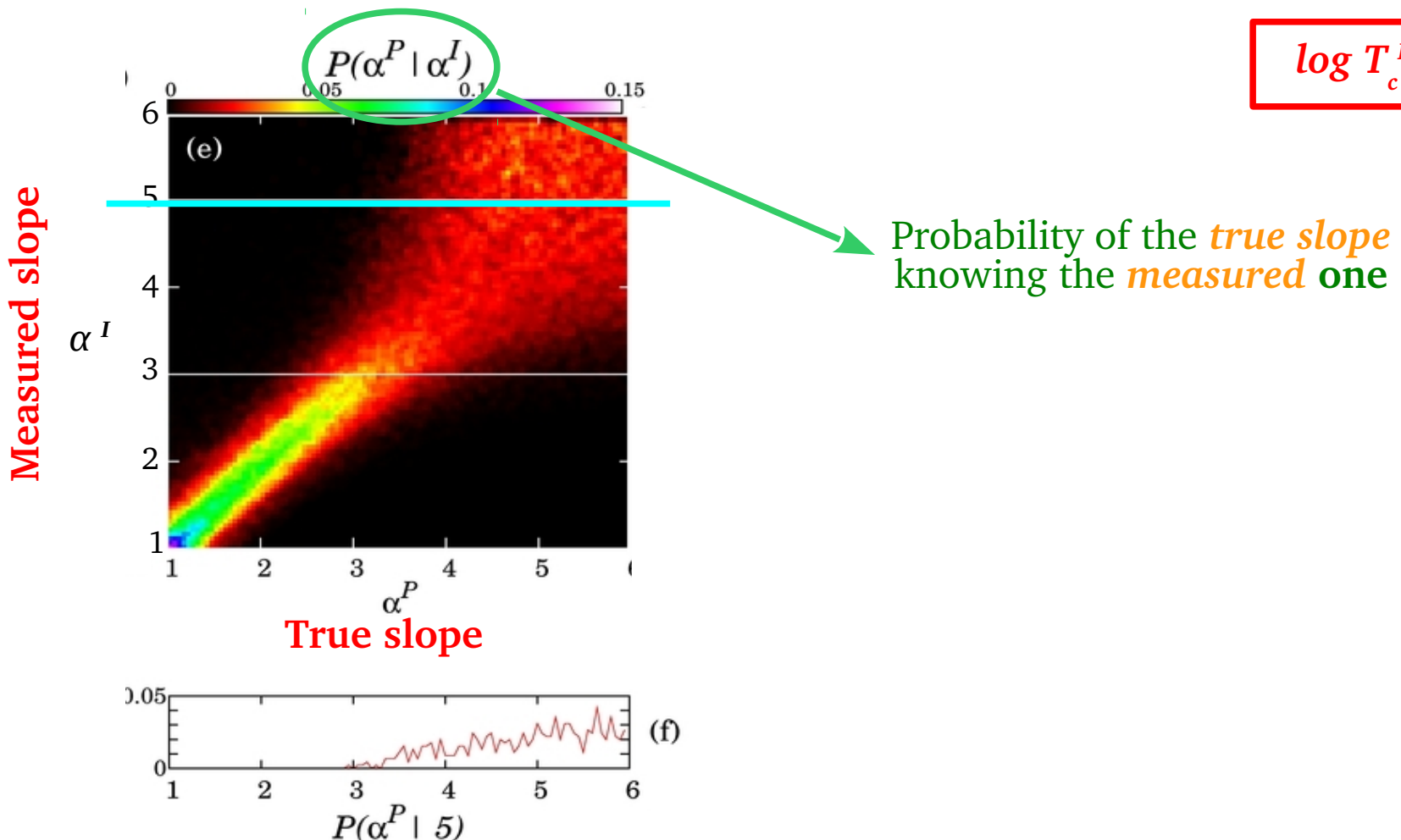
$$\log T_c^P = 6.8$$

## ■ Reconstruction of the slope

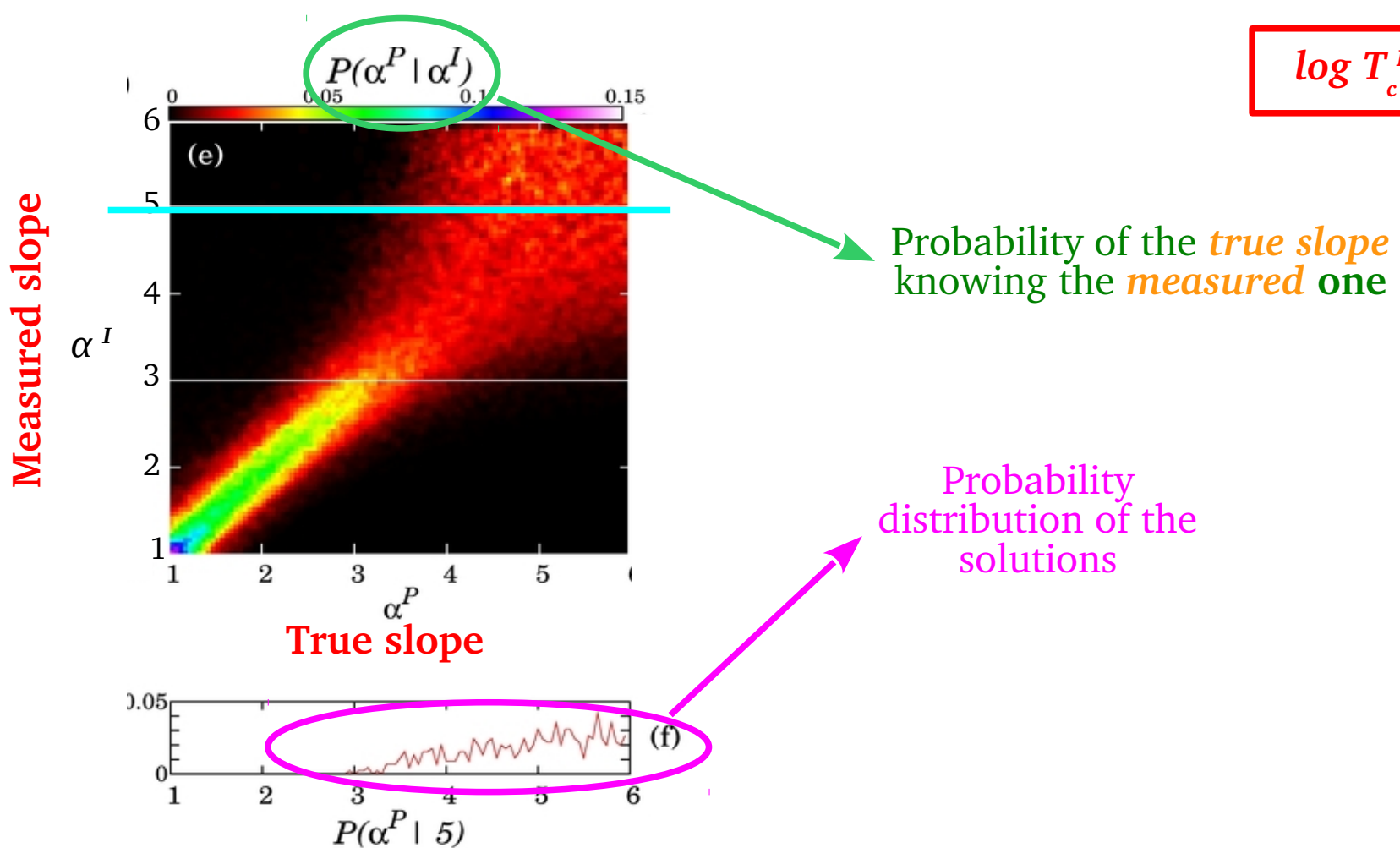


## ■ Reconstruction of the slope

$$\log T_c^P = 6.8$$



## ■ Reconstruction of the slope

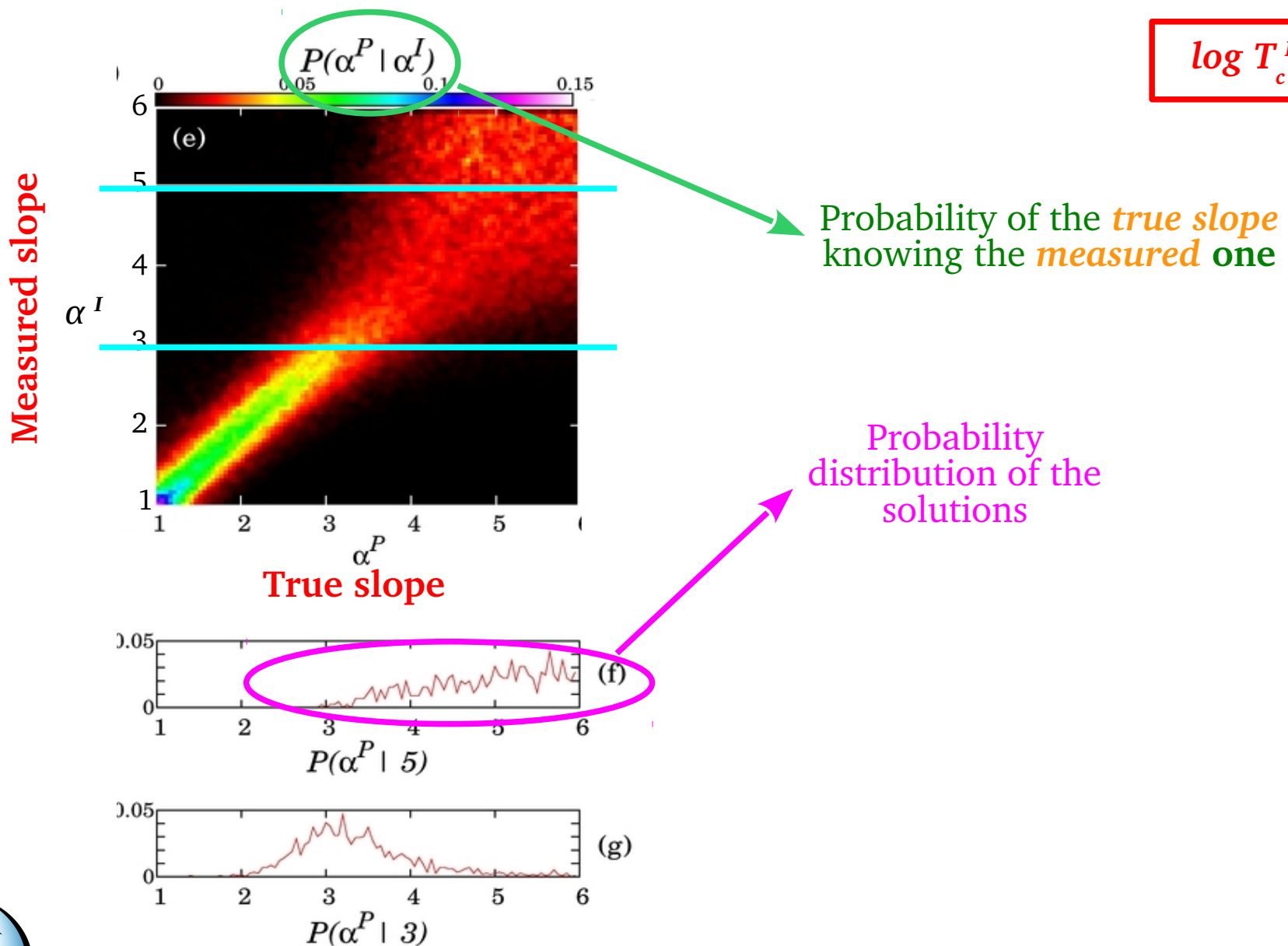


$$\log T_c^P = 6.8$$

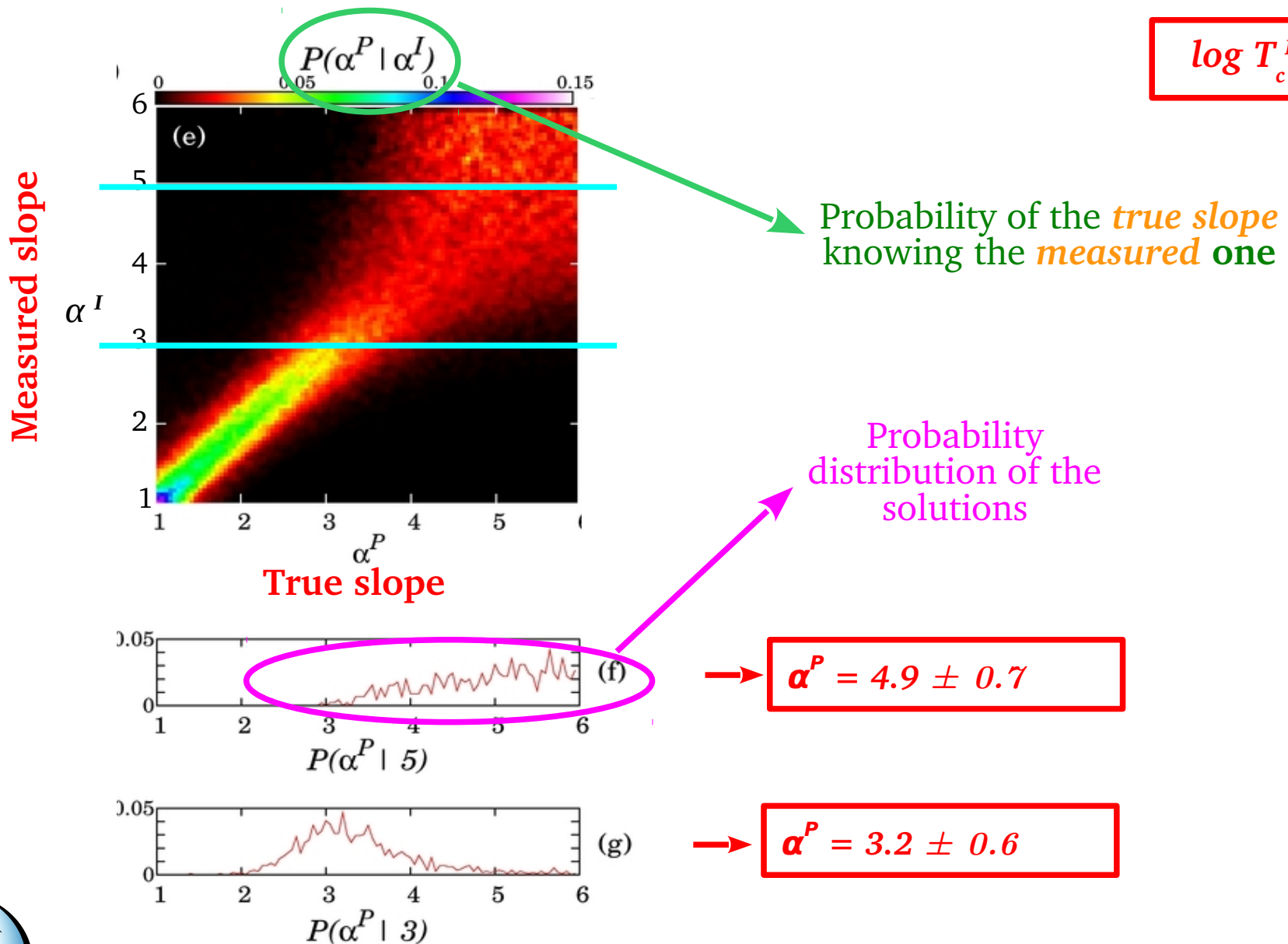
Probability of the *true slope*  
knowing the *measured* one

Probability  
distribution of the  
solutions

## ■ Reconstruction of the slope

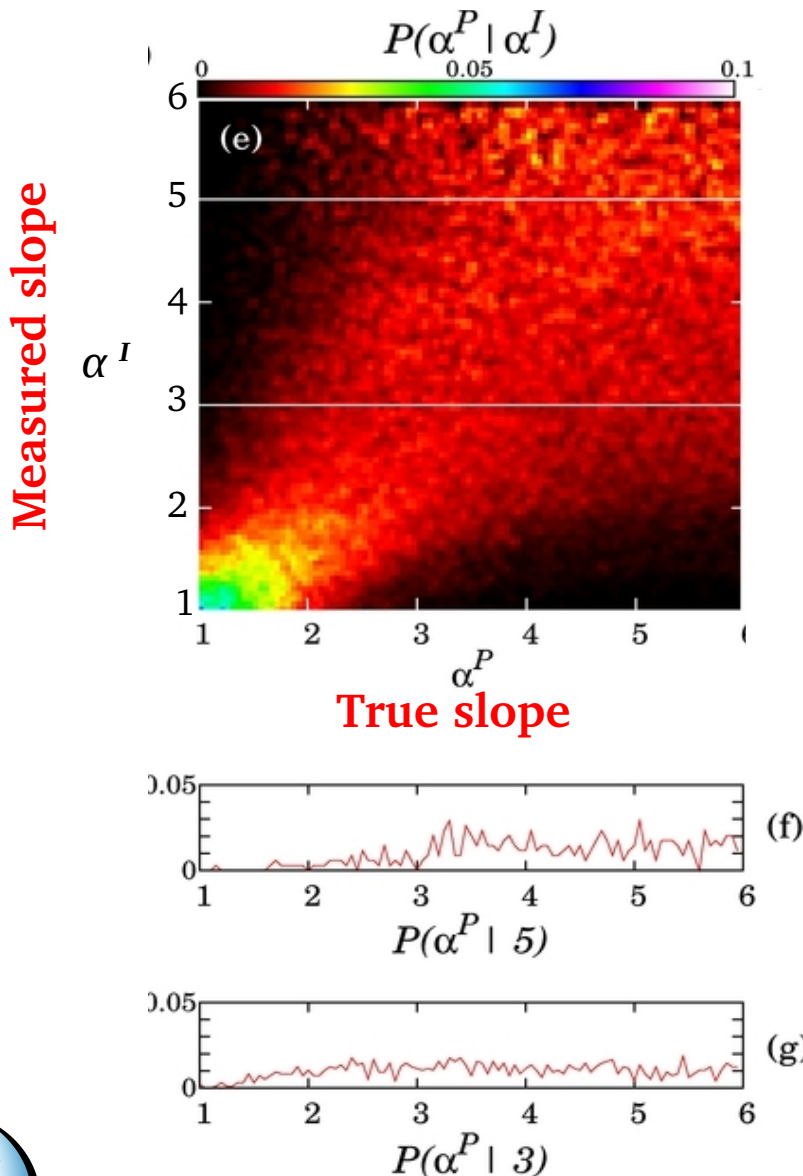


## ■ Reconstruction of the slope



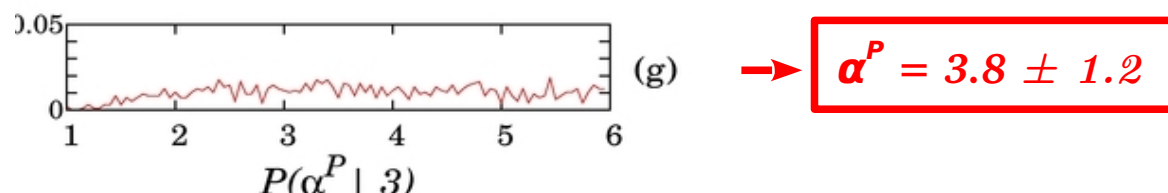
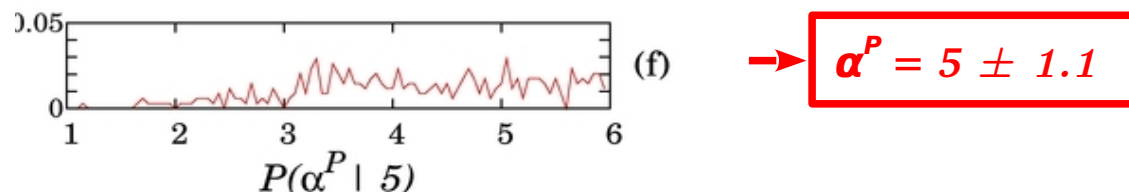
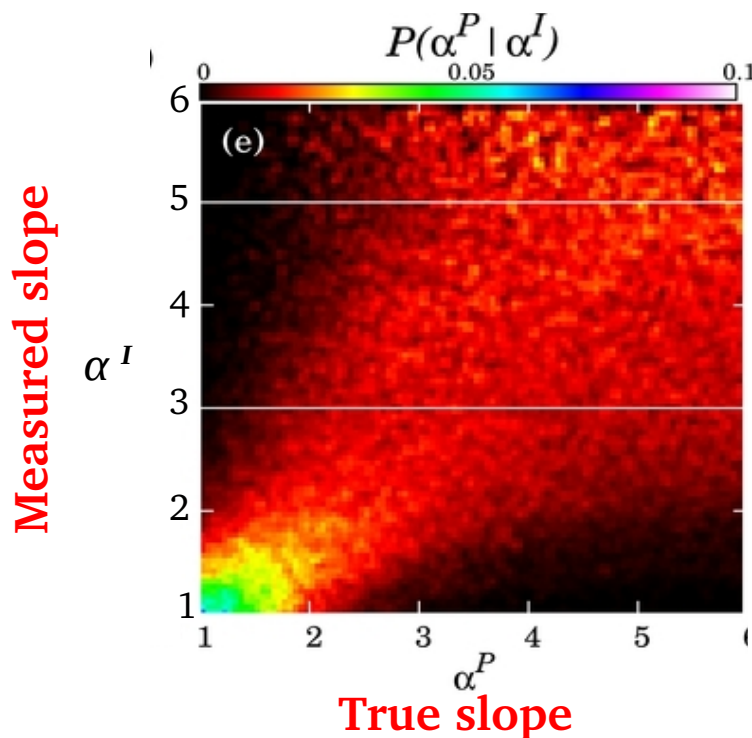
## ■ Reconstruction of the slope

$$\log T_c^P = 6.5$$

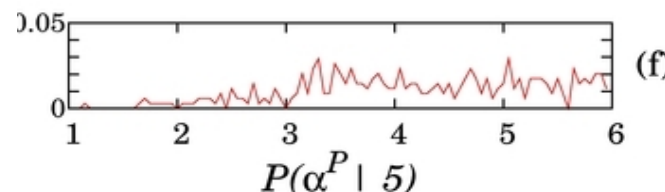
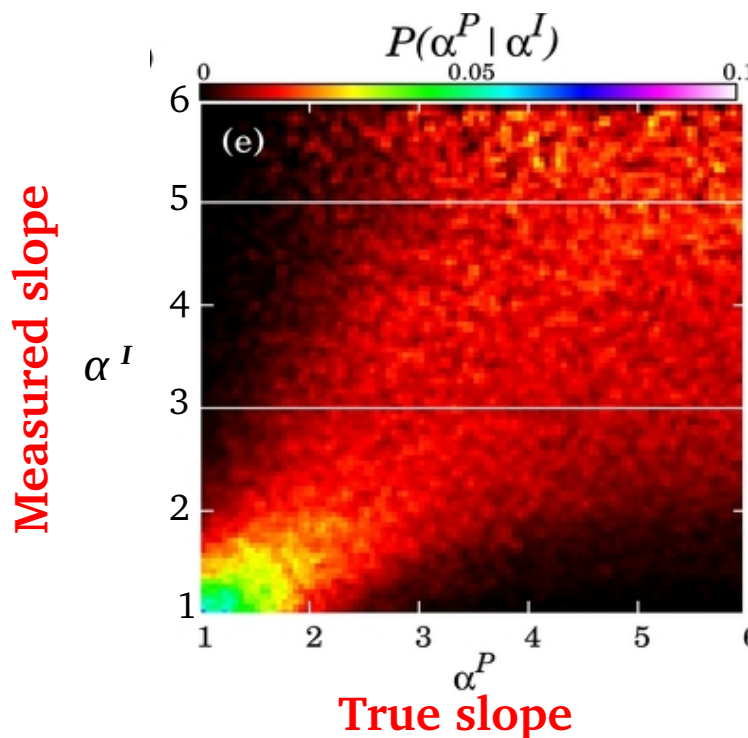


## ■ Reconstruction of the slope

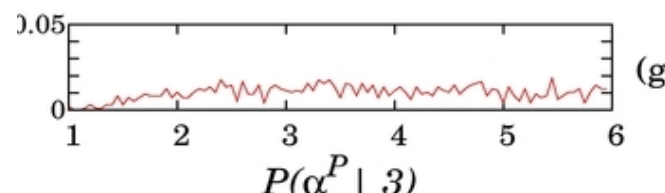
$$\log T_c^P = 6.5$$



## ■ Reconstruction of the slope

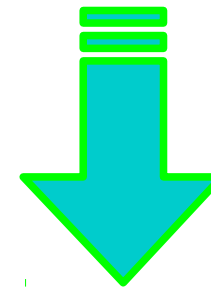


$$\rightarrow \alpha^P = 5 \pm 1.1$$



$$\rightarrow \alpha^P = 3.8 \pm 1.2$$

$$\log T_c^P = 6.5$$

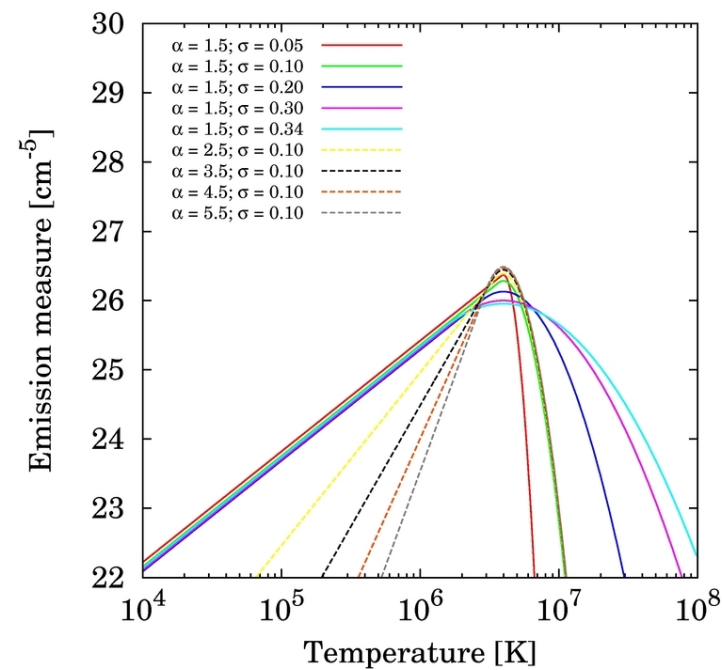


Dégradation of the quality  
of the reconstruction

## ■ List of used lines



Ions	Wavelength (Å)	$\log(T[K])$
Mg V	276.579	5.45
Mg VI	268.991	5.65
Mg VI	270.391	5.65
Si VII	275.354	5.80
Mg VII <sup>b</sup>	278.404	5.80
Mg VII	280.745	5.80
Fe IX	188.497	5.85
Fe IX	197.865	5.85
Fe X	184.357	6.05
Si IX	258.082	6.05
Fe XI	180.408	6.15
Fe XI	188.232	6.15
Si X	258.371	6.15
Si X	261.044	6.15
S X	264.231	6.15
Fe XII	192.394	6.20
Fe XII	195.119	6.20
Fe XIII	202.044	6.25
Fe XIII	203.828	6.25
Fe XIV	264.790	6.30
Fe XIV	270.522	6.30
Fe XIV <sup>b</sup>	274.204	6.30
Fe XV	284.163	6.35
S XIII <sup>b</sup>	256.685	6.40
Fe XVI	262.976	6.45
Ca XIV	193.866	6.55
Ca XV	200.972	6.65
Ca XVI	208.604	6.70
Ca XVII <sup>b</sup>	192.853	6.75

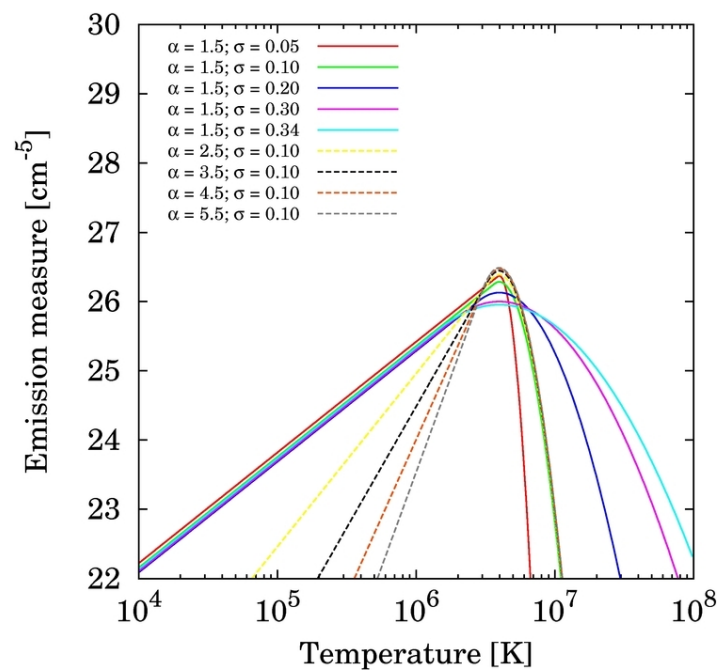


## ■ List of used lines



Ions	Wavelength (Å)	$\log(T[K])$
Mg V	276.579	5.45
Mg VI	268.991	5.65
Mg VII	270.391	5.65
Si VII	275.354	5.80
Mg VII <sup>b</sup>	278.404	5.80
Mg VII	280.745	5.80
Fe IX	188.497	5.85
Fe IX	197.865	5.85
Fe X	184.357	6.05
Si IX	258.082	6.05
Fe XI	180.408	6.15
Fe XI	188.232	6.15
Si X	258.371	6.15
Si X	261.044	6.15
S X	264.231	6.15
Fe XII	192.394	6.20
Fe XII	195.119	6.20
Fe XIII	202.044	6.25
Fe XIII	203.828	6.25
Fe XIV	264.790	6.30
Fe XIV	270.522	6.30
Fe XIV <sup>b</sup>	274.204	6.30
Fe XV	284.163	6.35
S XIII <sup>b</sup>	256.685	6.40
Fe XVI	262.976	6.45
Ca XIV	193.866	6.55
Ca XV	200.972	6.65
Ca XVI	208.604	6.70
Ca XVII <sup>b</sup>	192.853	6.75

$T_p = 10^{6.8} K$

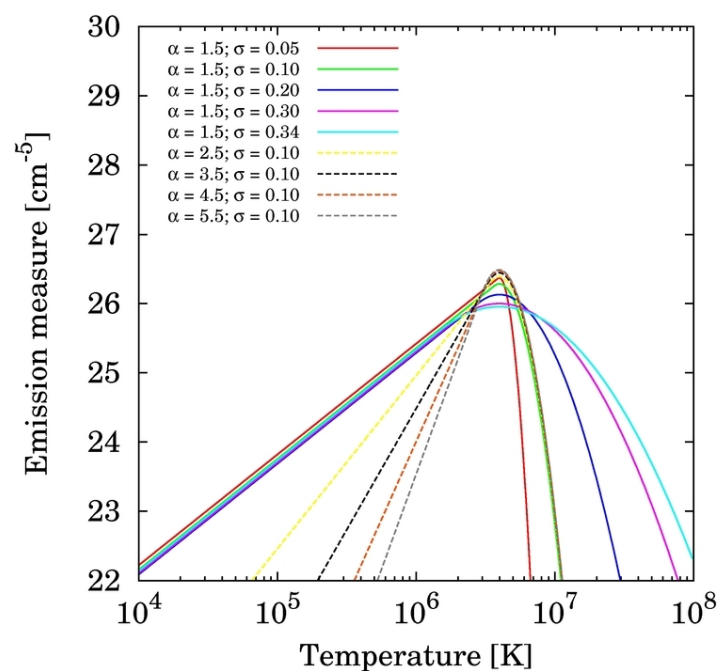


## ■ List of used lines

Ions	Wavelength (Å)	$\log(T[K])$
Mg V	276.579	5.45
Mg VI	268.991	5.65
Mg VI	270.391	5.65
Si VII	275.354	5.80
Mg VII <sup>b</sup>	278.404	5.80
Mg VII	280.745	5.80
Fe IX	188.497	5.85
Fe IX	197.865	5.85
Fe X	184.357	6.05
Si IX	258.082	6.05
Fe XI	180.408	6.15
Fe XI	188.232	6.15
Si X	258.371	6.15
Si X	261.044	6.15
S X	264.231	6.15
Fe XII	192.394	6.20
Fe XII	195.119	6.20
Fe XIII	202.044	6.25
Fe XIII	203.828	6.25
Fe XIV	264.790	6.30
Fe XIV	270.522	6.30
Fe XIV <sup>b</sup>	274.204	6.30
Fe XV	284.163	6.35
S XIII <sup>b</sup>	256.685	6.40
Fe XVI	262.976	6.45
Ca XIV	193.866	6.55
Ca XV	200.972	6.65
Ca XVI	208.604	6.70
Ca XVII <sup>b</sup>	192.853	6.75

$$T_p = 10^{6.5} K$$

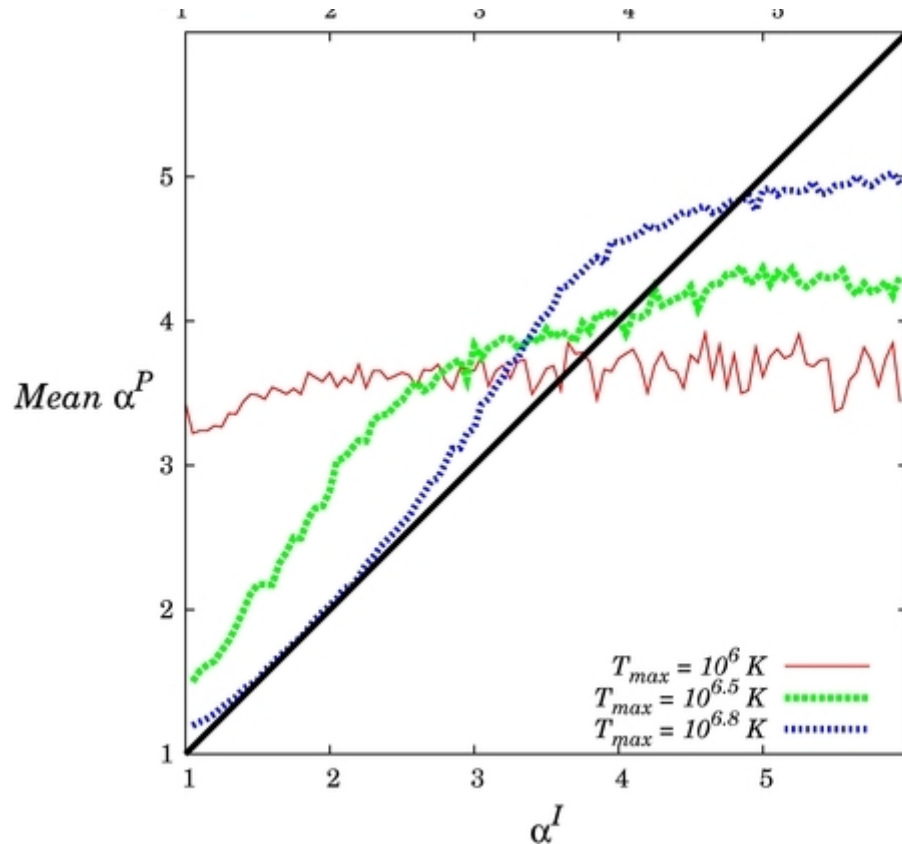
$$T_p = 10^{6.8} K$$



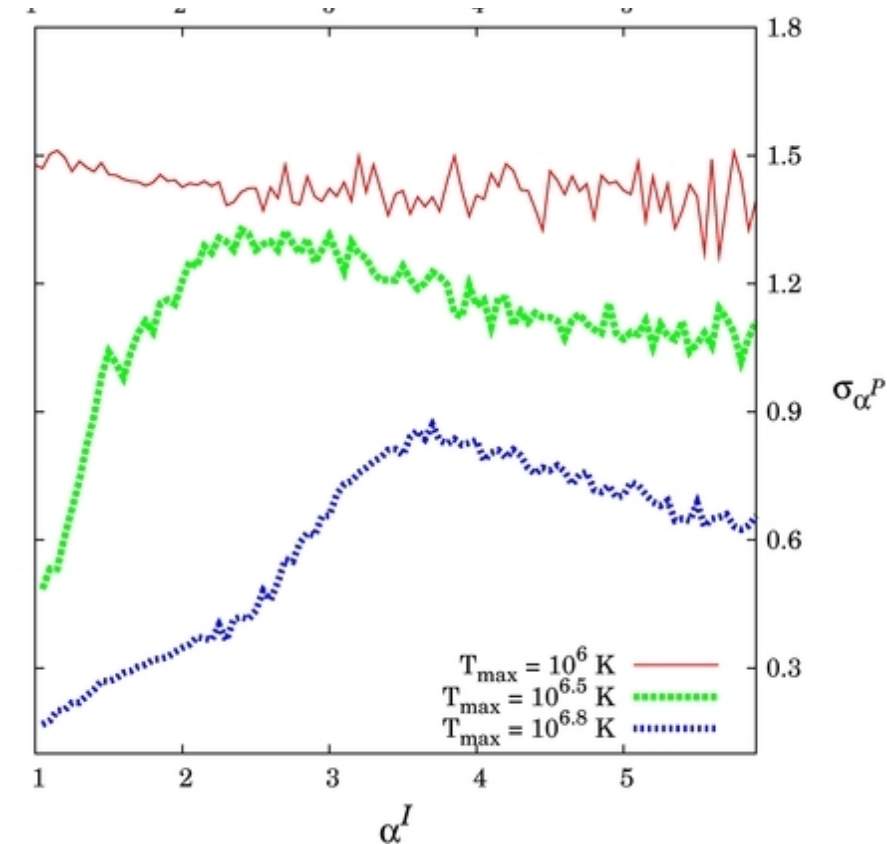
## ■ Providing confidence level on the DEM slope



True slope mean value



True slope standard deviation



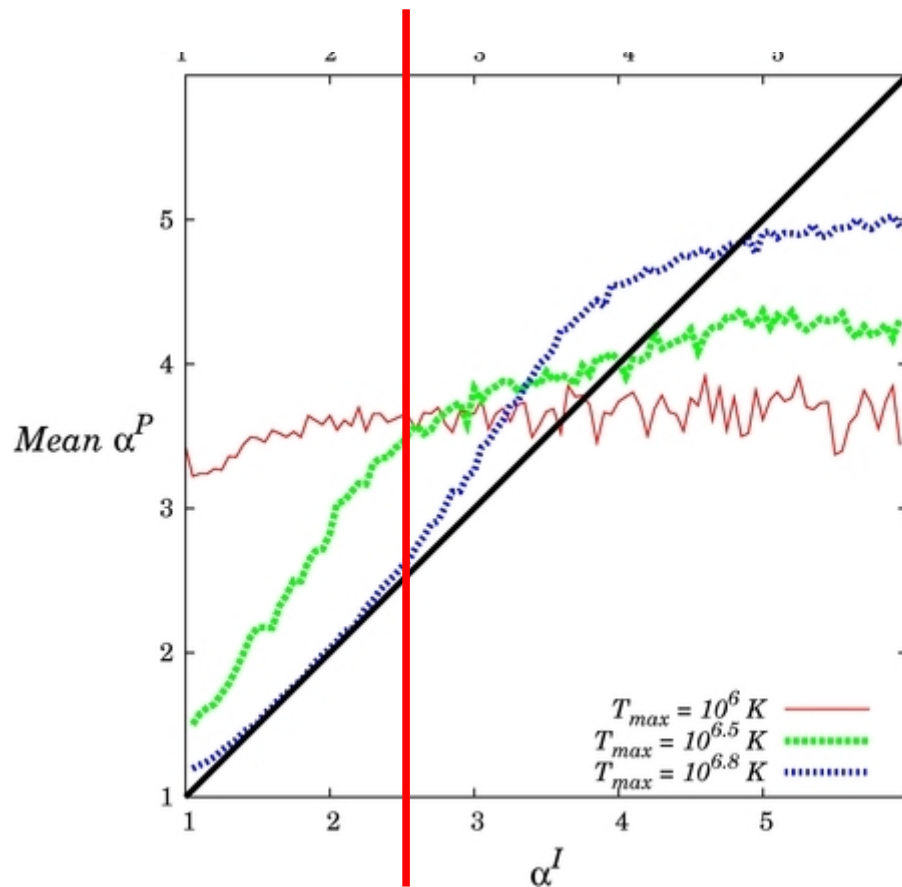
Measured slope

Measured slope

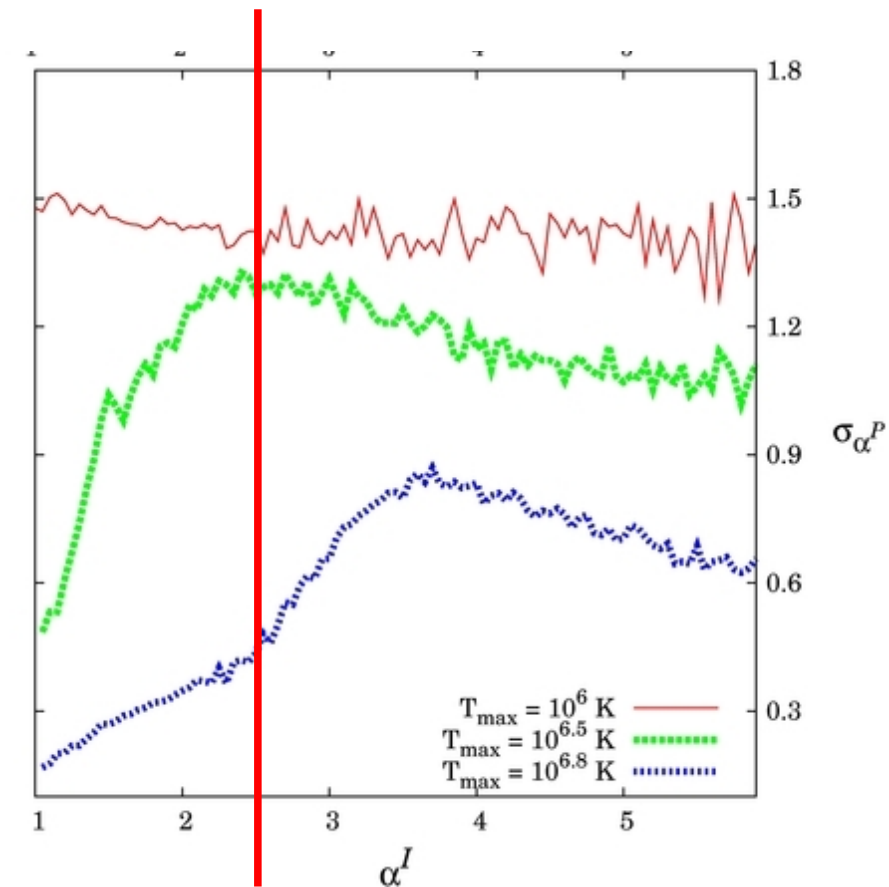
## ■ Providing confidence level on the DEM slope



True slope mean value



True slope standard deviation



Measured slope

Measured slope

## EIS capabilities



→ *Difficulty to constrain the timescale of heating event :*

**22 Active Region Cores (inter-moss regions)**

Bradshaw et al. (2012)

	$\alpha \leq 2.0$	$2.0 < \alpha \leq 2.5$	$2.5 < \alpha \leq 3.0$	$3.0 < \alpha \leq 3.5$	$\alpha > 3.5$
$\alpha$	3	5	3	6	5

Schmelz & Pathak (2012)  
Tripathi, Klimchuk, & Mason (2011)  
Warren, Brooks, & Winebarger (2011)  
Warren, Winebarger, & Brooks (2012)  
Winebarger et al. (2011)



# EIS capabilities

Introduction

I. Technique

II. Results

Conclusions

→ *Difficulty to constrain the timescale of heating event :*

**22 Active Region Cores (inter-moss regions)**

Bradshaw et al. (2012)

	$\alpha \leq 2.0$	$2.0 < \alpha \leq 2.5$	$2.5 < \alpha \leq 3.0$	$3.0 < \alpha \leq 3.5$	$\alpha > 3.5$
$\alpha$	3	5	3	6	5



Model of low frequency nanoflares →

**$0.81 \leq \alpha \leq 2.56$**



Schmelz & Pathak (2012)  
Tripathi, Klimchuk, & Mason (2011)  
Warren, Brooks, & Winebarger (2011)  
Warren, Winebarger, & Brooks (2012)  
Winebarger et al. (2011)

# EIS capabilities

Introduction

I. Technique

II. Results

Conclusions

→ *Difficulty to constrain the timescale of heating event :*

**22 Active Region Cores (inter-moss regions)**

Bradshaw et al. (2012)

	$\alpha \leq 2.0$	$2.0 < \alpha \leq 2.5$	$2.5 < \alpha \leq 3.0$	$3.0 < \alpha \leq 3.5$	$\alpha > 3.5$	
$\alpha$	3	5	3	6	5	<b>36% consistent</b>



Model of low frequency nanoflares →

$$0.81 \leq \alpha \leq 2.56$$



Schmelz & Pathak (2012)  
Tripathi, Klimchuk, & Mason (2011)  
Warren, Brooks, & Winebarger (2011)  
Warren, Winebarger, & Brooks (2012)  
Winebarger et al. (2011)

# EIS capabilities

Introduction

I. Technique

II. Results

Conclusions

→ *Difficulty to constrain the timescale of heating event :*

**22 Active Region Cores (inter-moss regions)**

Bradshaw et al. (2012)

$$\Delta\alpha = \pm 1.0$$

	$\alpha \leq 2.0$	$2.0 < \alpha \leq 2.5$	$2.5 < \alpha \leq 3.0$	$3.0 < \alpha \leq 3.5$	$\alpha > 3.5$	
$\alpha$	3	5	3	6	5	<b>36% consistent</b>



Model of low frequency nanoflares →

$$0.81 \leq \alpha \leq 2.56$$



Schmelz & Pathak (2012)  
Tripathi, Klimchuk, & Mason (2011)  
Warren, Brooks, & Winebarger (2011)  
Warren, Winebarger, & Brooks (2012)  
Winebarger et al. (2011)

# EIS capabilities

Introduction

I. Technique

II. Results

Conclusions

→ *Difficulty to constrain the timescale of heating event :*

**22 Active Region Cores (inter-moss regions)**

Bradshaw et al. (2012)

$$\Delta\alpha = \pm 1.0$$

	$\alpha \leq 2.0$	$2.0 < \alpha \leq 2.5$	$2.5 < \alpha \leq 3.0$	$3.0 < \alpha \leq 3.5$	$\alpha > 3.5$	
$\alpha$	3	5	3	6	5	<b>36% consistent</b>
$\alpha - \Delta\alpha$	11	6	2	2	1	<b>77% consistent</b>



Model of low frequency nanoflares →

$$0.81 \leq \alpha \leq 2.56$$



Schmelz & Pathak (2012)  
Tripathi, Klimchuk, & Mason (2011)  
Warren, Brooks, & Winebarger (2011)  
Warren, Winebarger, & Brooks (2012)  
Winebarger et al. (2011)

# EIS capabilities

Introduction

I. Technique

II. Results

Conclusions

→ *Difficulty to constrain the timescale of heating event :*

**22 Active Region Cores (inter-moss regions)**

Bradshaw et al. (2012)

$$\Delta\alpha = \pm 1.0$$

	$\alpha \leq 2.0$	$2.0 < \alpha \leq 2.5$	$2.5 < \alpha \leq 3.0$	$3.0 < \alpha \leq 3.5$	$\alpha > 3.5$	
$\alpha$	3	5	3	6	5	<b>36% consistent</b>
$\alpha - \Delta\alpha$	11	6	2	2	1	<b>77% consistent</b>
$\alpha + \Delta\alpha$			3	5	14	<b>0% consistent</b>



Model of low frequency nanoflares →

$$0.81 \leq \alpha \leq 2.56$$

Schmelz & Pathak (2012)  
Tripathi, Klimchuk, & Mason (2011)  
Warren, Brooks, & Winebarger (2011)  
Warren, Winebarger, & Brooks (2012)  
Winebarger et al. (2011)



# THANK YOU !



# List of used lines



Ion	Wavelength (Å)	$\log_{10} T$ (K)	Ion	Wavelength (Å)	$\log_{10} T$ (K)
Mg V	276.579	5.45	S X	264.231	6.15
Mg VI	268.991	5.65	Fe XII	192.394	6.20
Mg VI	270.391	5.65	Fe XII	195.119	6.20
Si VII	275.354	5.80	Fe XIII	202.044	6.25
Mg VII	278.404	5.80	Fe XIII	203.828	6.25
Mg VII	280.745	5.80	Fe XIV	264.790	6.30
Fe IX	188.497	5.85	Fe XIV	270.522	6.30
Fe IX	197.865	5.85	Fe XIV	274.204	6.30
Si IX	258.082	6.05	Fe XV	284.163	6.35
Fe X	184.357	6.05	S XIII	256.685	6.40
Fe XI	180.408	6.15	Fe XVI	262.976	6.45
Fe XI	188.232	6.15	Ca XIV	193.866	6.55
Si X	258.371	6.15	Ca XV	200.972	6.65
Si X	261.044	6.15	Ca XVI	208.604	6.70
S X	264.231	6.15	Ca XVII	192.853	6.75
			Fe XVII	269.494	6.75

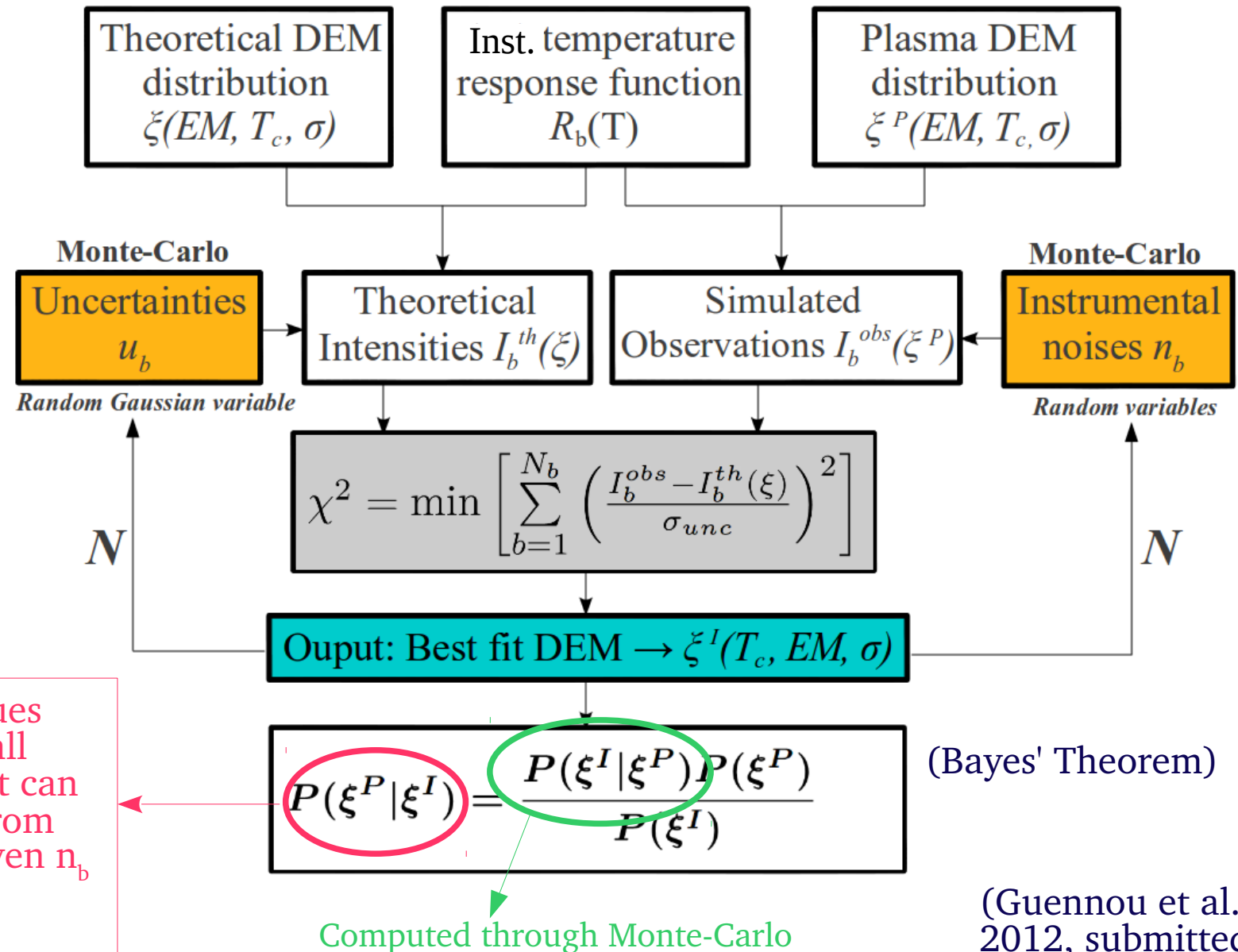


- Random and systematics errors are taken into account

Random $n_b$	Systematics $s_b$
Read noise	Calibration
Photon noise	Atomic physics



- {
- Abundance of each element : 30%
  - Ionization balance : 30%
  - combined radiative + excitation rates + atomic structure calculations uncertainties : 20%
  - FIP effect → 30% on low FIP elements





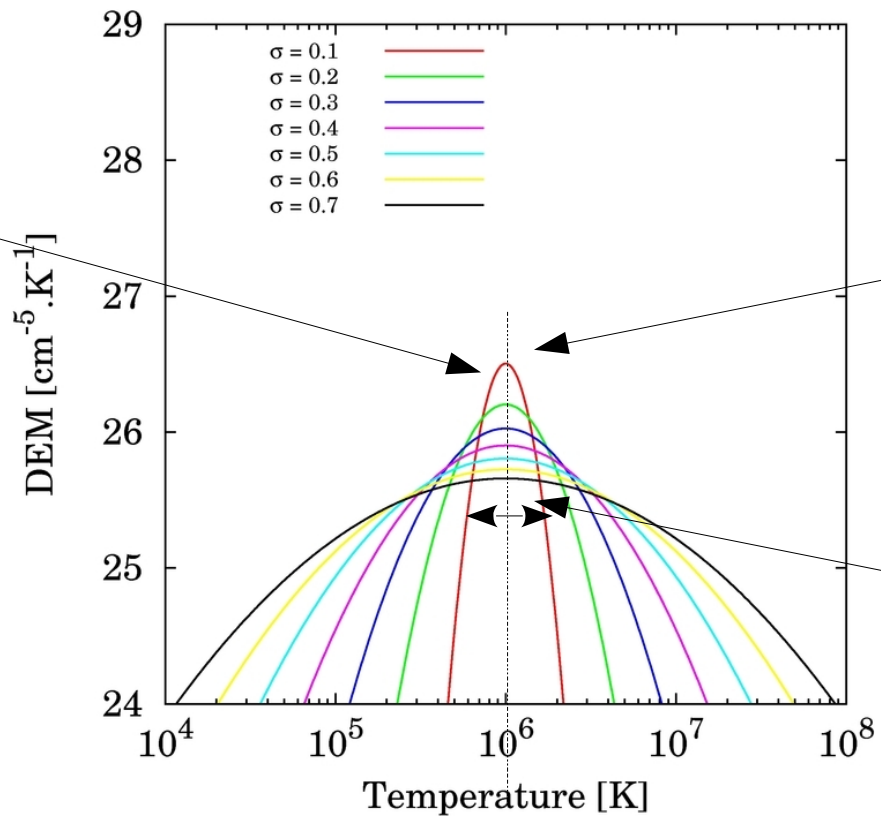
- EIS capabilities to reconstruct multithermal plasma
- Simulations using Gaussian DEMs  $\xi^P$ ,  
→ Useful to represent a great class of plasma thermal conditions

$$P(\mathbf{EM}^I, \mathbf{T}_c^I, \boldsymbol{\sigma}^I | \mathbf{EM}^P, \mathbf{T}_c^P, \boldsymbol{\sigma}^P)$$

●  $\mathbf{EM}^P$

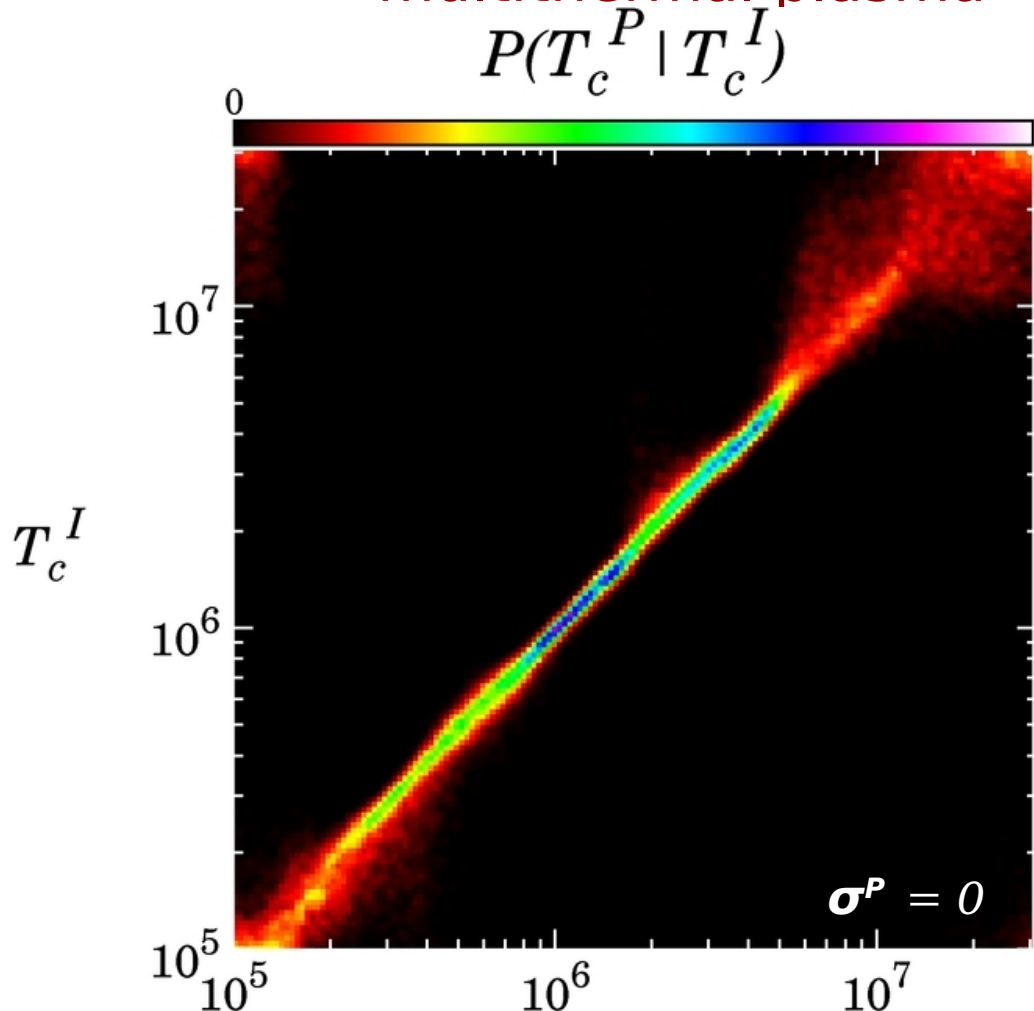
●  $\mathbf{T}_c^P$

●  $\boldsymbol{\sigma}^P$





- EIS capabilities to reconstruct multithermal plasma



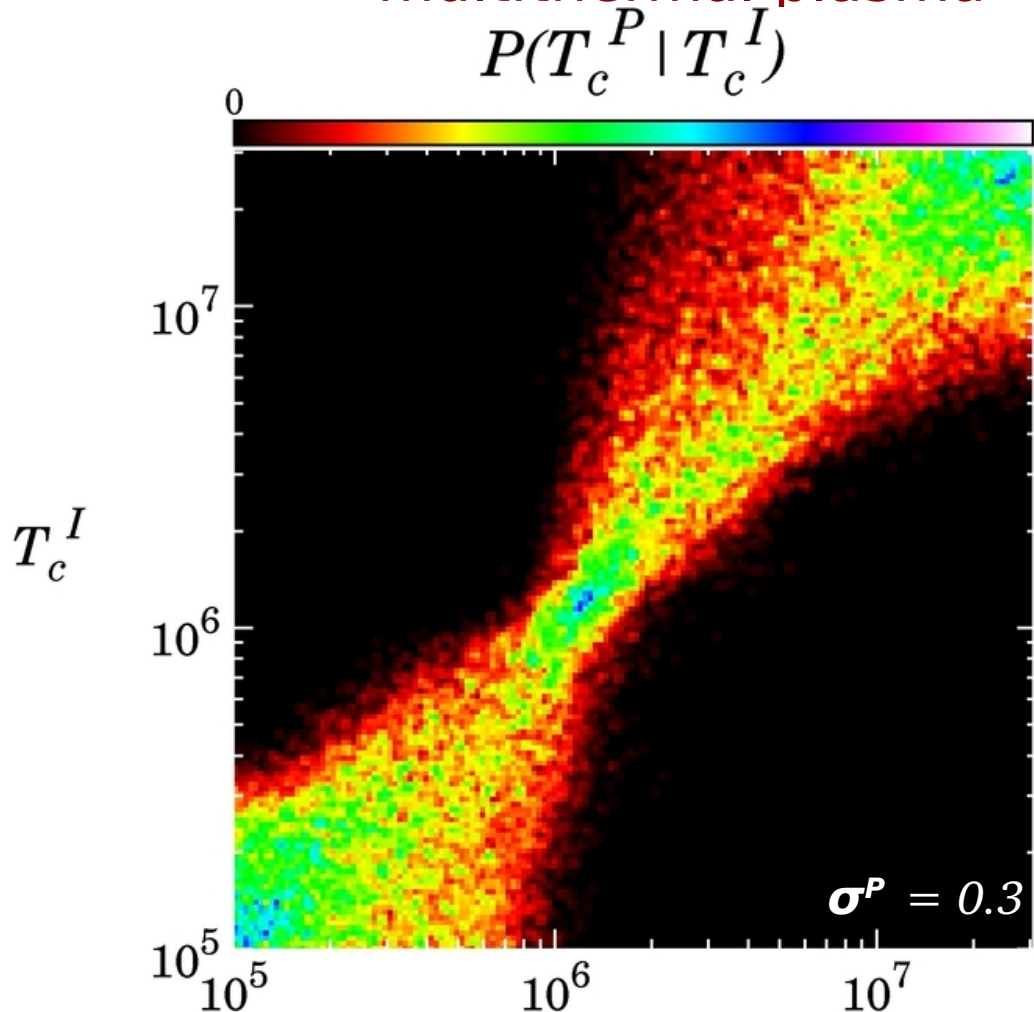
$$P(\mathbf{EM}^P, T_c^P, \sigma^P | \mathbf{EM}', T_c', \sigma')$$

- $\mathbf{EM}^P = 10^{28} \text{ m}^{-5}$

$$\Sigma(\mathbf{EM}', \sigma')$$



- EIS capabilities to reconstruct multithermal plasma



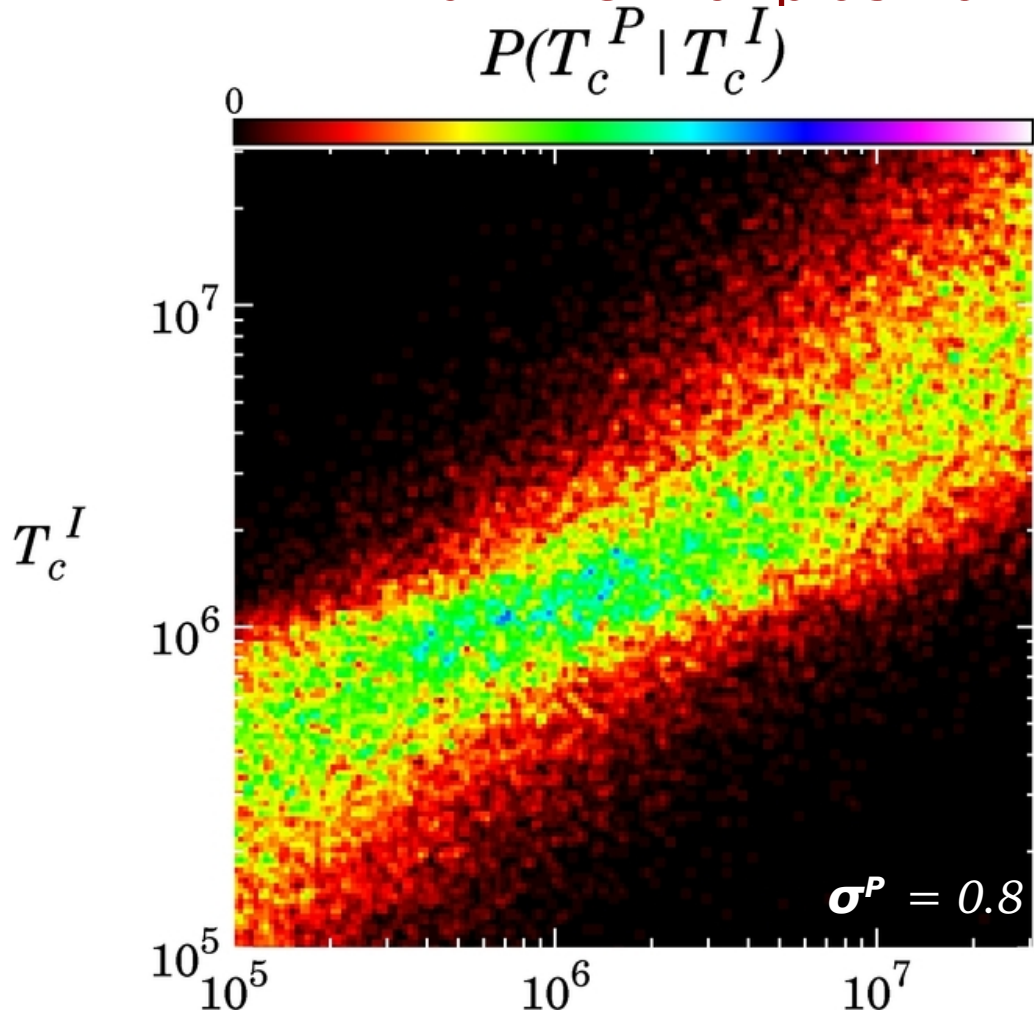
$$P(\mathbf{EM}^P, T_c^P, \sigma^P | \mathbf{EM}', T_c', \sigma')$$

●  $\mathbf{EM}^P = 10^{28} \text{ m}^{-5}$

$\Sigma(\mathbf{EM}', \sigma')$



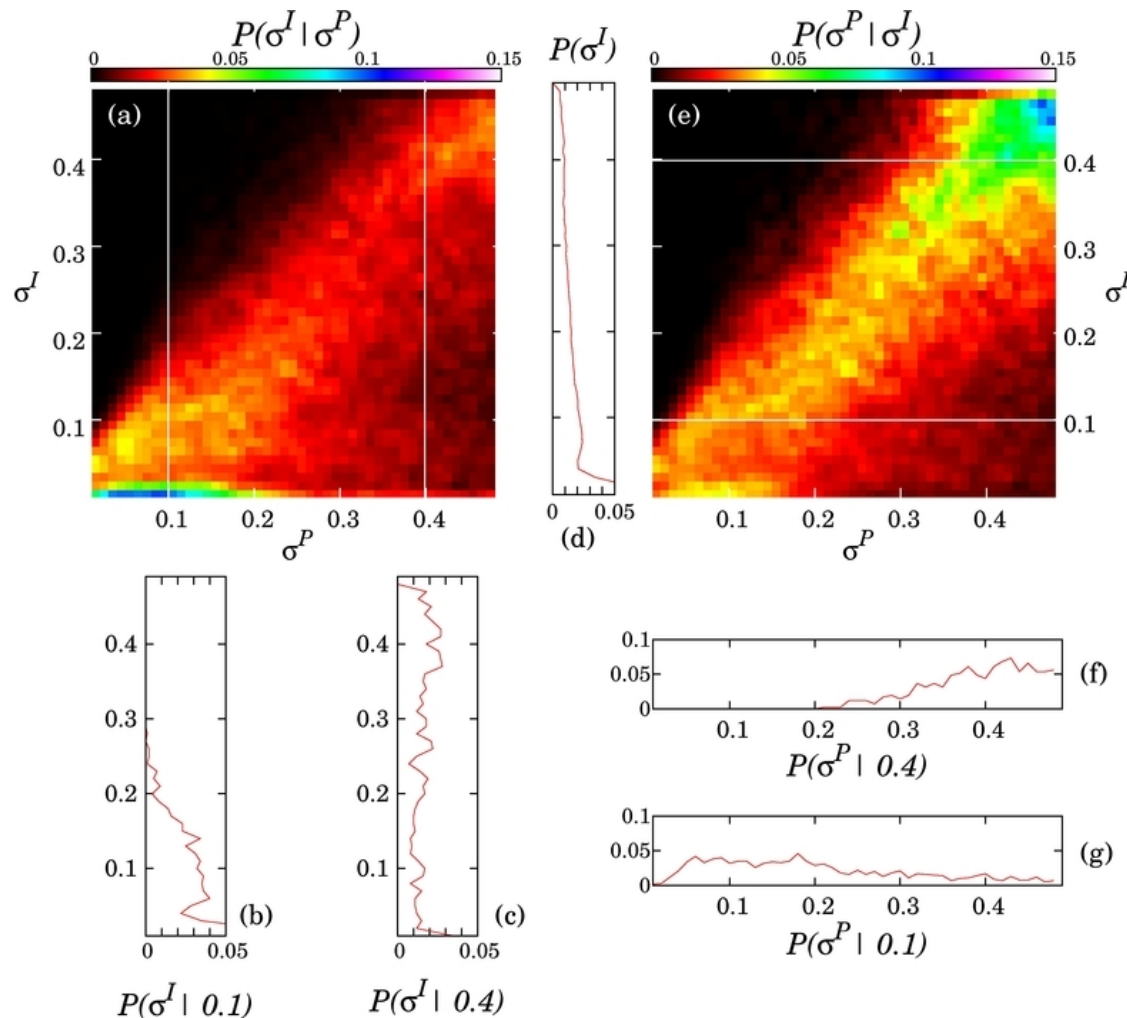
- EIS capabilities to reconstruct multithermal plasma



$$P(\mathbf{EM}^P, T_c^P, \sigma^P | \mathbf{EM}', T_c', \sigma')$$

- $\mathbf{EM}^P = 10^{28} \text{ m}^{-5}$

$$\Sigma(\mathbf{EM}', \sigma')$$



$T_p = 10^6 K$

→ Only a few information about the thermal structure at high temperature can be extracted (cf Winebarger et al. 2012)